Manganese Chalcogenides

International Edition: DOI: 10.1002/anie.201605410
German Edition: DOI: 10.1002/ange.201605410

Giant Pressure-Driven Lattice Collapse Coupled with Intermetallic Bonding and Spin-State Transition in Manganese Chalcogenides

Yonggang Wang[+], Ligang Bai[+], Ting Wen, Liuxiang Yang, Huiyang Gou, Yuming Xiao, Paul Chow, Michael Pravica, Wenge Yang,* and Yusheng Zhao**

Abstract: *Materials with an abrupt volume collapse of more than 20% during a pressure-induced phase transition are rarely reported. In such an intriguing phenomenon, the lattice may be coupled with dramatic changes of orbital and/or the spin-state of the transition metal. A combined in situ crystallography and electron spin-state study to probe the mechanism of the pressure-driven lattice collapse in MnS and MnSe is presented. Both materials exhibit a rocksalt-to-MnP phase transition under compression with ca. 22% unit-cell volume changes, which was found to be coupled with the $Mn^{2+}(d^5)$ spin-state transition from $S=5/2$ to $S=1/2$ and the formation of Mn−Mn intermetallic bonds as supported by the metallic transport behavior of their high-pressure phases. Our results reveal the mutual relationship between pressure-driven lattice collapse and the orbital/spin-state of Mn^{2+} in manganese chalcogenides and also provide deeper insights toward the exploration of new metastable phases with exceptional functionalities.*

As a common phenomenon in crystalline materials, phase transitions initiated by external temperature and pressure stimuli continue to attract intense interest for the opportunity to explore materials with novel structures and emerging physical properties.[1] Hydrostatic pressure, as an alternative to elemental substitution with different atomic sizes to generate chemical pressure, is the most appropriate route to modify the atomic distances gradually and thus change the chemical and physical properties of solids without introducing inhomogeneous disorder.[2] Under external forces, most of the materials follow the traditional expansion and contraction rule, that is, expansion upon heating and shrinking under compression. Nevertheless, there do exist a few materials displaying abnormal volume-change behaviors such as the negative thermal expansion (NTE)[3] and negative linear compressibility (NLC).[4] These phenomena are considered useful to achieve adjustable mechanical responses or stress of a given material by varying the composition and thus manipulate their physical properties.

More recently, scientists have been intrigued by materials with abnormal lattice-volume changes under high pressure. Duyker et al.[5] reported a series coordination frameworks $Ln(CN)_6$ (Ln = Ho, Lu, Y) with extreme compressibility. Under relatively low pressure (< 1 GPa), these materials exhibit the largest known pressure responses with a 20% reduction in volume through a torsion-gear mechanism based on rigid $Ln(CN)_6$ units. In some magnetic-metal-containing compounds such as YCo_5, SmS, and cerium metal, anomalous volume collapse has been associated with spin-state transitions due to the reduction of magnetic moment under high pressure.[6] These complex but interesting transitions provide a rare opportunity to study the fundamentals of chemical bonding and to understand the structural behaviors of the minerals inside Earth's crust and mantle.[7]

Manganese sulfides, MnS and MnS_2, despite their different structures (the former having a rocksalt structure and the latter a pyrite-type structure), have both been reported to undergo large volume collapses during pressure-induced phase transitions.[8,9] It is established that the structural stability of a compound subjected to high pressure depends not only on the crystal structure but also, to some extent, on the metal–ligand bonding strength especially when magneto-lattice coupling is involved in the phase transition. According to the hard–soft acid–base (HSAB) theory,[10] the stability sequence of manganese chalcogenides can be predicted as follows: MnO ≫ MnS > MnSe > MnTe. Thus, an interesting question arises as to whether heavy manganese chalcogenides also experience a large pressure-induced lattice collapse. On the other hand, both experimental and theoretical results on MnS and MnS_2 suggested that the spin-state transition of Mn^{2+} might play a significant role in the lattice collapse

[*] Dr. Y. Wang,[+] Prof. M. Pravica, Prof. Y. Zhao
High Pressure Science and Engineering Center
University of Nevada Las Vegas
Las Vegas, NV 89154 (USA)
E-mail: yyggwang@gmail.com
T. Wen
Institute of Nanostructured Functional Materials
Huanghe Science and Technology College
Zhengzhou, Henan 450006 (China)
Dr. Y. Wang,[+] Dr. L. Yang, W. Yang
High Pressure Synergetic Consortium (HPSynC)
Geophysical Laboratory, Carnegie Institution of Washington
Argonne, IL 60439 (USA)
Dr. L. Yang, H. Gou, W. Yang
Center for High Pressure Science and Technology Advanced Research (HPSTAR)
Shanghai 201203 (China)
E-mail: yangwg@hpstar.ac.cn
Dr. L. Bai,[+] Y. Xiao, P. Chow
High Pressure Collaborative Access Team (HPCAT)
Geophysical Laboratory, Carnegie Institution of Washington
Argonne, IL 60439 (USA)
Prof. Y. Zhao
Southern University of Science and Technology
Shenzhen, 518055 (China)
E-mail: zhaoys@sustc.edu.cn
[+] These authors contributed equally to this work.

Supporting information for this article can be found under: http://dx.doi.org/10.1002/anie.201605410.

process but without any direct evidence.[8,9] Herein, we present our results on the structural and Mn^{2+} spin-state behavior of MnS and MnSe under compression obtained by means of combined in situ synchrotron X-ray diffraction and X-ray emission spectroscopy. The first aim is to verify if the pressure-driven lattice collapse is universal in manganese chalcogenides. The other aim is to gain more insight into the interplay between lattice, orbital, and magnetism during such an abnormal phase transition.

In situ angle dispersive synchrotron X-ray diffraction (ADXRD) patterns of MnS and MnSe under high pressure were recorded at room temperature with an incident monochromatic wavelength of 0.4066 Å (for details, see the Supporting Information). Prominent structural transitions from the low-pressure (LP) phases to high-pressure (HP) phases occurred at approximately 30 GPa for MnS and started from approximately 20 GPa and completed at approximately 30 GPa for MnSe, respectively (Supporting Information, Figure S1). Referring to the structural analysis by Xiao et al.,[8] both materials possess the rocksalt-type structure at ambient conditions (cubic, $Pm\bar{3}m$), transform to the HP MnP-type phase (orthorhombic, *Pnma*), and remain stable up to the highest pressure points in our experiments (77.6 GPa for MnS and 47.4 GPa for MnSe). In the 20–30 GPa pressure range, there is an unknown intermediate phase (possibly with tetrahedral symmetry) existing between the LP and HP phases in MnSe. The ADXRD patterns can be well fitted and refined by using the ambient structures of MnS and MnSe for the LP phases and MnP for the HP phases as the starting models (Supporting Information, Figure S2). Figure 1 shows the fitting results of the cell volumes of MnS and MnSe versus applied pressure. Notably, the unit cell volume decreases dramatically by about 22 % from the LP rocksalt phases to the HP MnP-type phases, dominating the *P–V* profiles and indicating the occurrence of first-order phase transitions with remarkable changes of the atomic arrangement. Considering that for most of the other materials a 5 % volume collapse during a phase transition has been regarded as notable,[9,11] such giant pressure-driven lattice collapses are

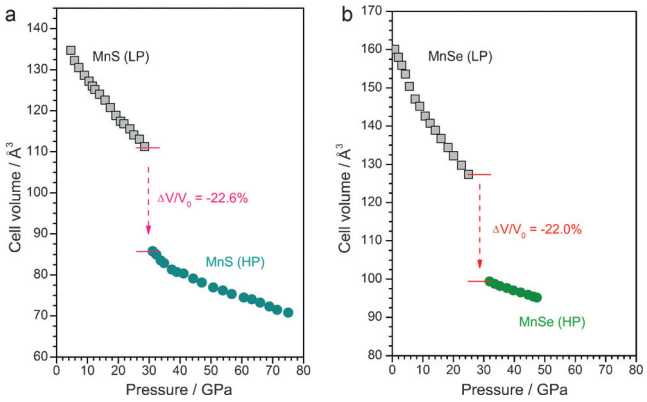

Figure 1. Experimental cell volumes as a function of applied pressure for the LP and HP phases of a) MnS and b) MnSe. The fitting of the *P–V* data according to the third-order Birch–Murnaghan equation-of-state functions gives bulk modulus B_0 (LP) = 72, B_0 (HP) = 80 GPa for MnS, and B_0 (LP) = 68, B_0 (HP) = 218 GPa for MnSe, respectively.

novel and merit more investigations on their origin. Similar volume collapses of transition-metal-containing minerals have been supposed to occur in the Earth's mantle.[7] Moreover, the HP phase of MnS and MnSe with MnP-type structure exhibits a much smaller compressibility than that of their LP phases (with bulk moduli $B_0 = 80.0$ and 218.0 GPa for the HP MnS and MnSe phases versus $B_0 = 72.0$ and 68.0 GPa for the LP phases, respectively).

Figure 2 shows the crystal structures of the LP and HP phases of MnS and MnSe. The LP phase adopts a cubic

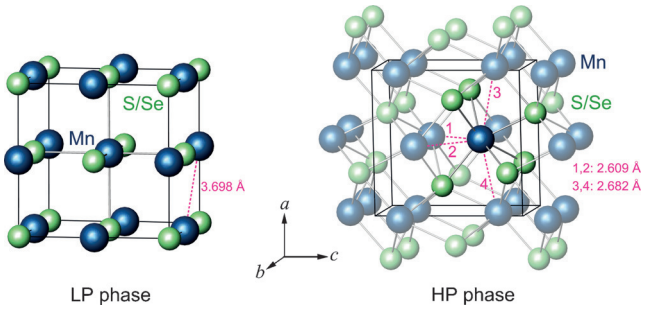

Figure 2. Illustration of the crystal structures for the LP ($Pm\bar{3}m$) and HP (*Pnma*) phases of MnS and MnSe (Mn, blue; S/Se, cyan). The distorted $Mn(S,Se)_6$ octahedron is highlighted in the HP structure and the shortest or the near-shortest Mn–Mn bond lengths are shown by dashed lines. The schematic bond-length values are taken from the MnS structures at ambient conditions and 31.2 GPa, respectively.

rocksalt structure in which all of the Mn atoms coordinate with six S/Se atoms in an undistorted octahedral geometry. The $Mn(S,Se)_6$ octahedra share their edges with the shortest Mn–Mn distance of 3.698 Å (MnS) at ambient conditions. On the other hand, in the HP MnP-type structure, the $Mn(S,Se)_6$ octahedra are highly distorted and face-shared with two of their neighbors. This leads to the formation of two Mn–Mn intermetallic bonds with a length of 2.682 Å (derived from the refined structure of MnS at 31.2 GPa, and the corresponding Mn–S/Se bond lengths under compression are shown in the the Supporting Information, Figure S3). There are two other short Mn–Mn intermetallic bonds, each 2.609 Å, formed due to the substantial squeezing of Mn–(S/Se)–Mn bond angles under high pressure. The formation of the metallic Mn–Mn bonds is considered to be an incidental event during the giant pressure-driven lattice collapse of manganese chalcogenides. It is interesting to compare the cases of MnS/MnSe with that of MnS_2,[9] where Mn–Mn metallic bonds form dimers to stabilize the HP structure, and the semiconductor character is preserved in the high-pressure phase. In HP phases of MnS/MnSe, all of the Mn atoms are connected by Mn–Mn metallic bonds to form a three dimensional network (Supporting Information, Figure S4). We measured the transport behavior of MnSe as a function of pressure (*R–P*) and temperature (*R–T*) (see the Supporting Information). The metallization of MnSe observed under high pressure accompanied with the LP-to-HP phase transition can further verify the rationality of the HP MnP-type structure (see the Supporting Information, Figure S5). Recently, Cheng et al.[12] reported the emerging superconductivity of MnP under high pressure as the first

example of an Mn-based superconductor. Inevitably, it is highly expected that HP MnS/MnSe, which has the same crystal structure as MnP, may also become superconducting under high pressure. Experiments on this supposition are in progress.

Nevertheless, the formation of the Mn–Mn metallic bonds is merely a consequence of the giant lattice collapse of MnS and MnSe. The original driving force should be the pressure-induced spin-state transitions of Mn^{2+}, that is, from high spin ($S=5/2$) to low spin ($S=1/2$). To verify this hypothesis directly, pressure-dependent X-ray emission spectroscopy (XES) investigations of MnS and MnSe were conducted at the 16 ID-D beamline at HPCAT (for details, see the Supporting Information). Figure 3 presents the Mn K_β XES

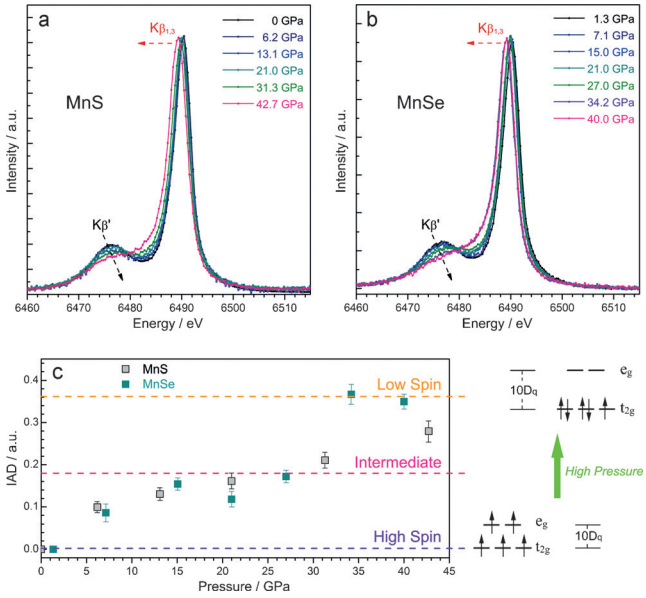

Figure 3. Mn K_β XES of a) MnS and b) MnSe as a function of applied pressure. c) The integrals of the absolute values of the difference spectra (IAD) obtained relative to the lowest spectra for MnS and MnSe as a function of pressure. The color lines are guides for the eye showing the evolution from high and intermediate to low-spin states. Note that the further splitting of e_g and t_{2g} orbits in distorted $Mn(S,Se)_6$ octahedra is disregarded in the diagram for brevity.

spectra of MnS and MnSe under compressions of up to 40 GPa, above the pressures where the phase transitions of MnS and MnSe occur. The Mn K_β' peaks decrease gradually for both MnS and MnSe with increase in pressure, and the Mn $K_{\beta1,3}$ lines shift to the lower energy sides correspondingly. Both results indicate the spin-state suppression of Mn^{2+} under pressure, that is, from the high-spin state to the low-spin state.

Following the procedure described by Vankó et al.,[13] quantitative analysis of the XES data has been conducted using the integrals of the absolute values of the difference spectra (IAD). The spectra were normalized first with respect to the areas and then shifted to have centers of mass at the same position. In this case, the IAD values reflect a linear relationship with the average spin numbers. Figure 3c shows the pressure dependence of the Mn^{2+} spin state in MnS/MnSe from the IAD analysis. The starting materials at ambient conditions have high Mn^{2+} spin states with $S=5/2$ (IAD = 0). As the pressure increases, the IAD value increases gradually indicating a pressure-induced gradual decrease of the Mn^{2+} magnetic moment. In the 15–30 GPa range, both materials may exhibit an intermediate spin state with $S=3/2$. When the applied pressure exceeds the LP–HP phase transition points, the IAD falls into the $S=1/2$ low-spin state level rapidly which indicates a complete landslide of the Mn^{2+} moments. It is well-known that the spin state of a given transition metal ion depends on the competition of the crystal field splitting energy ($10D_q$) and the electronic Coulomb repulsion. However, it is obvious that the external pressure affects the crystal field splitting energy more markedly than the latter in the case of manganese chalcogenides. Thus the ambient high-spin state of Mn^{2+} ($t_{2g}^3e_g^2$), stabilized by Hund's rule, is broken down to a $t_{2g}^5e_g^0$ low-spin state under high pressure. This leads to the symmetry-breaking of the crystalline lattice to distorted $Mn(S,Se)_6$ octahedra and the formation of dense MnP-type phases. On the other hand, the dramatic decrease of Mn^{2+} ionic size from 0.83 Å to 0.67 Å caused by the high-spin to low-spin transition[14] will also induce a geometric mismatch between Mn–Mn and Mn–(S/Se) bond lengths in the rocksalt phases and finally lead to the formation of Mn–Mn intermetallic bonds.

In summary, we observed the giant lattice collapse of manganese chalcogenides MnS and MnSe during the pressure-induced phase transition from rocksalt-type to MnP-type structures. Based on in situ structural analyses and XES evidence, dramatic orbital and spin-state changes were directly observed during the phase transition, that is, the formation of Mn–Mn intermetallic bonds and the Mn^{2+} spin state from high-spin ($S=5/2$) to low-spin ($S=1/2$). Our results provide a deeper understanding of the relationship between pressure-driven lattice collapse and the orbital/spin-state of transition metal ions in manganese chalcogenides, which may accelerate the exploration and structural design of novel functional materials.

Experimental Section

MnS and MnSe powders were purchased from Alfa-Aesar without further purification. For the in situ high-pressure measurements, a symmetrical diamond anvil cell (DAC) was employed to generate high pressure. Neon was used as the pressure-transmitting medium (PTM), and the pressures were determined by the ruby fluorescence method. A focused monochromatic X-ray beam with a diameter of approximately 3 μm (FWHM) and a wavelength of 0.4066 Å was used for the diffraction experiments, and the ADXRD patterns were recorded with a two-dimensional area PILATUS detector. For the high-pressure X-ray emission spectroscopy (XES) experiments, Be gaskets were used as the sample chamber and silicone oil was used as PTM. Electrical resistance was measured by a four-point-probe resistance measurement system. A cubic boron nitride layer was inserted into the DAC between the steel gasket and diamond anvil to provide electrical insulation between the electrical leads and gasket. Four gold wires were arranged to contact the sample in the chamber for resistance measurement. For details, see the Supporting Information.

Acknowledgements

This work was supported by the DOE-BES X-ray Scattering Core Program under grant number DE-FG02-99ER45775. The UNLV High Pressure Science and Engineering Center (HiPSEC) is a DOE-NNSA Center of Excellence supported by Cooperative Agreement DE-NA0001982. HPCAT operations are supported by DOE-NNSA under Award No. DE-NA0001974 and DOE-BES under Award No. DE-FG02-99ER45775, with partial instrumentation funding by NSF. APS is supported by DOE-BES, under Contract No. DE-AC02-06CH11357. Y.W. also thanks the support from the National Natural Science Foundation of China (21301063).

Keywords: high pressure · intermetallic bonding · lattice collapse · manganese chalcogenides · spin-state transitions

How to cite: *Angew. Chem. Int. Ed.* **2016**, *55*, 10350–10353
Angew. Chem. **2016**, *128*, 10506–10509

[1] a) T. Vicsek, A. Czirók, E. Ben-Jacob, I. Cohen, O. Shochet, *Phys. Rev. Lett.* **1995**, *75*, 1226–1229; b) B. A. Bernevig, T. L. Hughes, S.-C. Zhang, *Science* **2006**, *314*, 1757–1761; c) S. T. Martin, *Chem. Rev.* **2000**, *100*, 3403–3453; d) X. Moya, S. Kar-Narayan, N. D. Mathur, *Nat. Mater.* **2014**, *13*, 439–450; e) M. Shatruk, H. Phan, B. A. Chrisostomo, A. Suleimenova, *Coord. Chem. Rev.* **2015**, *289–290*, 62–73.

[2] a) P. F. McMillan, *Nat. Mater.* **2002**, *1*, 19–25; b) Y. Ma, M. Eremets, A. R. Oganov, Y. Xie, I. Trojan, S. Medvedev, A. O. Lyakhov, M. Valle, V. Prakapenka, *Nature* **2009**, *458*, 182–186.

[3] a) T. A. Mary, J. S. O. Evans, T. Vogt, A. W. Sleight, *Science* **1996**, *272*, 90–92; b) J. S. O. Evans, *J. Chem. Soc. Dalton Trans.* **1999**, 3317–3326; c) A. L. Goodwin, M. Calleja, M. J. Conterio, M. T. Dove, J. S. O. Evans, D. A. Keen, L. Peters, M. G. Tucker, *Science* **2008**, *319*, 794–797; d) B. K. Greve, K. L. Martin, P. L. Lee, P. J. Chupas, K. W. Chapman, A. P. Wilkinson, *J. Am. Chem. Soc.* **2010**, *132*, 15496–15498; e) X. Song, Z. Sun, Q. Huang, M. Rettenmayr, X. Liu, M. Seyring, G. Li, G. Rao, F. Yin, *Adv. Mater.* **2011**, *23*, 4690–4694; f) S. G. Duyker, V. K. Peterson, G. J. Kearley, A. J. Ramirez-Cuesta, C. J. Kepert, *Angew. Chem. Int. Ed.* **2013**, *52*, 5266–5270; *Angew. Chem.* **2013**, *125*, 5374–5378.

[4] a) R. H. Baughman, S. Stafström, C. Cui, S. O. Dantas, *Science* **1998**, *279*, 1522–1524; b) A. L. Goodwin, D. A. Keen, M. G. Tucker, *Proc. Natl. Acad. Sci. USA* **2008**, *105*, 18708–18713; c) W. Li, M. R. Probert, M. Kosa, T. D. Bennett, A. Thirumurugan, R. P. Burwood, M. Parinello, J. A. K. Howard, A. K. Cheetham, *J. Am. Chem. Soc.* **2012**, *134*, 11940–11943; d) A. B. Cairns, J. Catafesta, C. Levelut, J. Rouquette, A. van der Lee, L. Peters, A. L. Thompson, V. Dmitriev, J. Haines, A. L. Goodwin, *Nat. Mater.* **2013**, *12*, 212–216; e) W. Cai, A. Gładysiak, M. Anioła, V. J. Smith, L. J. Barbour, A. Katrusiak, *J. Am. Chem. Soc.* **2015**, *137*, 9296–9301.

[5] S. G. Duyker, V. K. Peterson, G. J. Kearley, A. J. Studer, C. J. Kepert, *Nat. Chem.* **2016**, *8*, 270–275.

[6] a) P. W. Bridgman, *Proc. Am. Acad. Arts Sci.* **1927**, *62*, 207–226; b) P. W. Bridgman, *Proc. Am. Acad. Arts Sci.* **1948**, *76*, 55–70; c) A. Chatterjee, A. K. Singh, A. Jayaraman, *Phys. Rev. B* **1972**, *6*, 2285–2291; d) H. Rosner, D. Koudela, U. Schwarz, A. Handstein, M. Hanfland, I. Opahle, K. Koepernik, M. D. Kuz′min, K.-H. Müller, J. A. Mydosh, M. Richter, *Nat. Phys.* **2006**, *2*, 469–472.

[7] a) R. E. Cohen, I. I. Mazin, D. G. Isaak, *Science* **1997**, *275*, 654–657; b) J.-F. Lin, T. Tsuchiya, *Phys. Earth Planet. Inter.* **2008**, *170*, 248–259.

[8] G. Xiao, X. Yang, X. Zhang, K. Wang, X. Huang, Z. Ding, Y. Ma, G. Zou, B. Zou, *J. Am. Chem. Soc.* **2015**, *137*, 10297–10303.

[9] S. A. J. Kimber, A. Salamat, S. R. Evans, H. O. Jeschke, K. Muthukumar, M. Tomić, F. Salvat-Pujol, R. Valentí, M. V. Kaisheva, I. Zizak, T. Chatterji, *Proc. Natl. Acad. Sci. USA* **2014**, *111*, 5106–5110.

[10] a) R. G. Pearson, *J. Am. Chem. Soc.* **1963**, *85*, 3533–3539; b) R. G. Parr, R. G. Pearson, *J. Am. Chem. Soc.* **1983**, *105*, 7512–7516.

[11] a) J. Kuneš, A. V. Lukoyanov, V. I. Anisimov, R. T. Scalettar, W. Pickett, *Nat. Mater.* **2008**, *7*, 198–202; b) J. W. Allen, R. M. Martin, *Phys. Rev. Lett.* **1982**, *49*, 1106–1110; c) P. Vajeeston, P. Ravindran, R. Vidya, H. Fjellvåg, A. Kjekshus, *Phys. Rev. B* **2003**, *68*, 212101; d) A. Kreyssig, M. A. Green, Y. Lee, G. D. Samolyuk, P. Zajdel, J. W. Lynn, S. L. Budko, M. S. Torikachvili, N. Ni, S. Nandi, J. B. Leão, S. J. Poulton, D. N. Argyriou, B. N. Harmon, R. J. McQueeney, P. C. Canfield, A. I. Goldman, *Phys. Rev. B* **2008**, *78*, 184517; e) W. Xiao, D. Tan, X. Xiong, J. Liu, J. Xu, *Proc. Natl. Acad. Sci. USA* **2010**, *107*, 14026–14029.

[12] J.-G. Cheng, K. Matsubayashi, W. Wu, J. P. Sun, F. K. Lin, J. L. Luo, Y. Uwatako, *Phys. Rev. Lett.* **2015**, *114*, 117001.

[13] G. Vankó, T. Neisius, G. Molná, F. Renz, S. Kárpáti, A. Shukla, F. M. F. de Groot, *J. Phys. Chem. B* **2006**, *110*, 11647–11653.

[14] R. D. Shannon, *Acta Crystallogr. Sect. A* **1976**, *32*, 751–767.

Received: June 3, 2016
Published online: July 27, 2016

